Supporting Information

for

Benzoate Ester as a New Species for Supramolecular Chiral Assembly

Chuanqiang Zhou,[a] *Qianqian Xu,*[b] *Yuanyuan Ren,*[a] *Xiaohuan Sun,* [b] *Zhilong Xu,*[b] *Jie Han,*[*, b] *Rong Guo* [b]

[a]Testing Center, Yangzhou University, Yangzhou City, Jiangsu, 225002, P. R. China

[a]School of Chemistry and Chemical Engineering, Yangzhou University, Yangzhou, Jiangsu, 225002, P. R. China

E-mail addresses: hanjie@yzu.edu.cn

Contents

Table S1 Elemental compositions of DMNDB. The measured element values are basically identical to these theoretical values according to its molecular formula ($C_{56}H_{94}O_4$).

Sample	C (wt%)	H (wt%)	O(wt%)
Extractive studied in this work	80.77	11.28	7.95
Theoretical values of tetramer $C_{56}H_{94}O_4$	80.96	11.33	7.71

Molecular simulation data

Molecular structure of DMNDB is shown as follow:

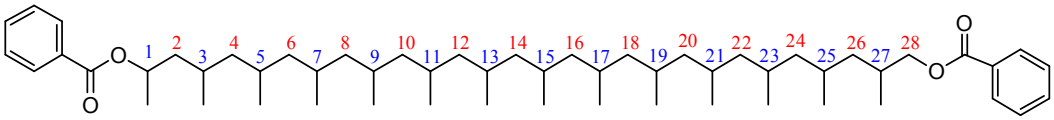

In the molecule chain, there are 14 CH_3 groups at odd C atoms in the spacer. As for every CH_3 group, two possible configurations could be listed as follow:

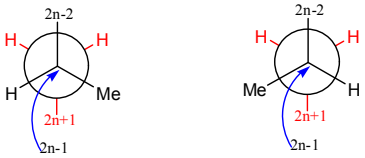

So, there are 2^{14}=16384 configurations which might present in the sample according to the positions of CH_3 groups. To estimate the most reasonable configurations, DMNDB molecule could be simplified to a short-chained and similar molecule as follow:

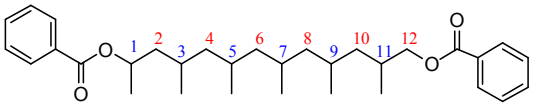

According to the positions of CH_3 groups, three typical configurations could be considered to simulate the optimized conformation at B3LYP/6-31G* EM=GD3BJ level, and the results are listed as follow:

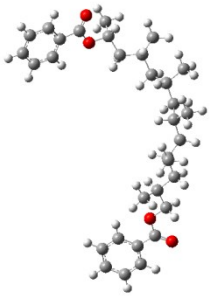

RRRRRR

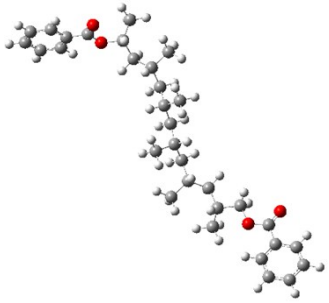

RRRLLL

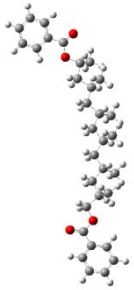

RLRLRL

Table S2 Calculation results of molecular energy of 12 chained molecule in consideration of positions of CH_3 groups simulated at B3LYP/6-31G* EM=GD3BJ level.

	E_{elec} (a.u.)*	**RE** (kcal/mol)*	**E_{elec}(+ZPE)** (a.u.) *	**RE(+ZPE)** (kcal/mol) *
RRRRRR	-1548.21925695	9.653	-1547.492376	10.057
RRRLLL	-1548.22265151	7.522	-1547.495994	7.787
RLRLRL	-1548.23463934	0.000	-1547.508403	0.000

*E_{elec}: Electron energy; RE: relative energy; E_{elec}(+ZPE): Electron energy corrected to zero-point energy; RE(+ZPE): relative energy corrected to zero-point energy;

Evidently, RLRLRL configuration should be the optimized one due to the lowest RE(+ZPE) values. On the basis of RLRLRL configuration in the spacer, the heading (C1) and ending (C12) benzoate COC_6H_5 groups could change their position to obtain different configurations, for example:

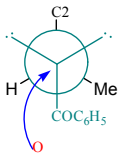

A1

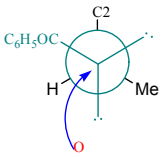

A2

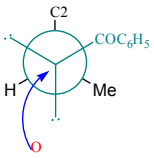

A3

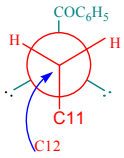

B1

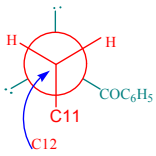

B2

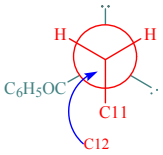

B3

Table S3 Calculation results of molecular energy of 12 chained molecule in consideration of positions of CH_3 and benzoate COC_6H_5 groups simulated at B3LYP/6-31G* EM=GD3BJ level.

		E_{elec} (a.u.)*	RE (kcal/mol)*	E_{elec}(+ZPE) (a.u.)*	RE(+ZPE) (kcal/mol) *
A1	B1	-1548.23463934	0.742	-1547.508403	0.474
	B2	-1548.23568044	0.088	-1547.509090	0.043
A2	B1	-1548.23477074	0.659	-1547.508483	0.424
	B2	-1548.23582139	0.000	-1547.509159	0.000
A3	B1	-1548.23130846	2.832	-1547.504870	2.691
	B2	-1548.23232377	2.195	-1547.505534	2.275

From the above result, one could find that A2B2 configuration should be the optimized one due to the little RE(+ZPE) value. According to A2B2 configuration, three typical configurations for DMNDB molecule could be considered to simulate the optimized conformation at B3LYP/6-31G* EM=GD3BJ level, and the results are listed as follow:

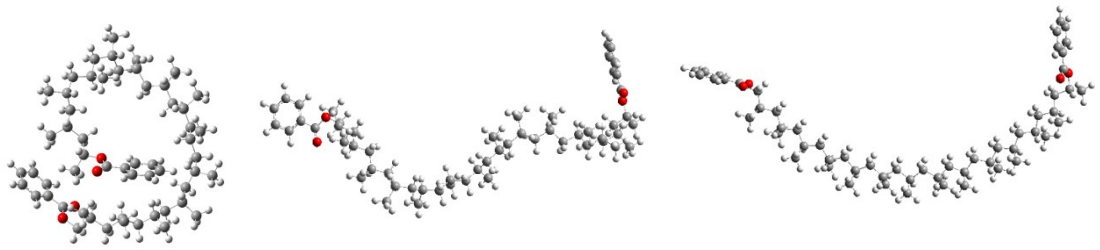

R14 R7L7 RL7

The above three configurations are calculated at two levels of B3LYP/6-31G* EM=GD3BJ and M062X/Def2SVP EM=GD3 to estimate the optimized conformation, and the results is listed as follows:

Table S4 Calculation results of molecular energy of DMNDB in consideration of positions of CH_3 groups simulated at B3LYP/6-31G* EM=GD3BJ level.

	E_{elec} (a.u.)	RE (kcal/mol)	E_{elec}+ZPE (a.u.)	RE(+ZPE) (kcal/mol)	G (a.u.) *	RG (kcal/mol) *
R14	-	6.489	-2490.457084	8.567	-	18.303
R7L7	-	22.445	-2490.433280	23.504	-	25.403
RL7	-	0.000	-2490.470736	0.000	-	0.000

*G: Gibbs free energy; RG: relative Gibbs free energy.

Table S5 Calculation results of molecular energy of DMNDB in consideration of positions of CH_3 groups simulated at M062X/Def2SVP EM=GD3 level.

	E_{elec}(a.u.)	RE (kcal/mol)	E_{elec}+ZPE (a.u.)	RE(+ZPE) (kcal/mol)	G (a.u.) *	RG (kcal/mol) *
R14	-	11.051	-2487.139030	12.805	-2487.247757	20.721
R7L7	-	23.803	-2487.119554	25.026	-2487.240033	25.568
RL7	-	0.000	-2487.159436	0.000	-2487.280778	0.000

From Table S3 and S4, the R7L7 configuration should be unstable one with large RG value, thus, only R14 and RL7 configurations are further considered to estimate the effect of the position of the COC_6H_5 groups.

Table S6 Calculation results of molecular energy of R14 configuration of DMNDB molecule in consideration of positions of CH_3 and benzoate COC_6H_5 groups simulated at B3LYP/6-31G* EM=GD3BJ level.

	R14		E_{elec} (a.u.)	RE (kcal/mol)	E_{elec}+ZPE (a.u.)	RE(+ZPE) (kcal/mol)	G (a.u.)	RG (kcal/mol)
A1	B1	1*	-	15.126	-2490.476556	14.700	-	12.038
		2*	-	9.999	-2487.161642	9.744	-	9.116
		3*	-	13.242	-2487.161015	13.680	-	12.466
	B2	1*	-	2.811	-2490.495104	3.061	-	3.506
		2*	-	14.506	-2487.153877	14.617	-	11.874
		3*	-	3.442	-2487.176023	4.263	-	5.201
	B3	1*	-	4.385	-2490.493379	4.143	-	3.891
		2*	-	15.878	-2487.152750	15.325	-	10.672
		3*	-	3.645	-2487.176563	3.924	-	4.086
A2	B1	1*	-	0.000	-2490.499982	0.000	-	0.000
		2*	-	0.000	-2487.177171	0.000	-	0.000
		3*	-	0.000	-2487.182816	0.000	-	0.000
	B2	1*	-	27.117	-2490.457084	26.919	-	23.842
		2*	-	13.146	-2487.156490	12.978	-	9.991
		3*	-	26.966	-2487.139030	27.476	-	24.064
	B3	1*	-	9.157	-2490.485051	9.369	-	8.711
		2*	-	10.281	-2487.161111	10.078	-	7.091
		3*	-	8.398	-2487.168055	9.263	-	10.314
A3	B1	1*	-	7.498	-2490.487937	7.558	-	7.506
		2*	-	26.920	-2487.134376	26.854	-	22.398
		3*	-	7.414	-2487.170149	7.949	-	8.866
	B2	1*	-	5.757	-2490.490777	5.776	-	5.466
		2*	-	19.576	-2487.146830	19.039	-	14.343
		3*	-	7.096	-2487.171282	7.238	-	7.769
	B3	1*	-	0.510	-2490.498592	0.872	-	1.745
		2*	-	30.046	-2487.129574	29.868	-	25.058
		3*	-	0.287	-2487.181329	0.933	-	2.883

Number represents different calculation methods: 1: B3LYP/6-31G EM=GD3BJ; 2: M062X/Def2SVP EM=GD3; 3: B3LYP/6-31G* EM=GD3BJ→M062X/Def2SVP EM=GD3.

Table S7 Calculation results of molecular energy of RL7 configuration of DMNDB molecule in consideration of positions of CH_3 and benzoate COC_6H_5 groups simulated at B3LYP/6-31G* EM=GD3BJ level.

RL7			E_{elec} (a.u.)	RE (kcal/mol)	E_{elec}+ZPE (a.u.)	RE(+ZPE) (kcal/mol)	G (a.u.)	ΔG (kcal/mol)
A1	B1	1	-	0.715	-	0.449	-	0.439
		2	-	0.562	-	0.398	-	0.644
	B2	1	-	0.079	-	0.040	-	0.414
		2	-	0.000	-	0.000	-	0.000
	B3	1	-	0.710	-	0.671	-	0.701
		2	-	0.702	-	0.930	-	1.790
A2	B1	1	-	0.641	-	0.401	-	0.438
		2	-	0.779	-	0.732	-	1.175
	B2	1	-	0.000	-	0.000	-	0.000
		2	-	0.236	-	0.493	-	1.199
	B3	1	-	0.634	-	0.624	-	1.192
		2	-	0.926	-	1.042	-	1.682
A3	B1	1	-	2.811	-	2.642	-	2.897
		2	-	2.429	-	2.504	-	3.414
	B2	1	-	2.177	-	2.255	-	3.013
		2	-	1.881	-	2.143	-	3.145
	B3	1	-	2.803	-	2.819	-	3.422
		2	-	2.565	-	2.926	-	4.460

Subsequently, configurations and molecular energies of both R14 and RL7 in mixed solvents (THF/W=3：7 and IPA(i-propanol)/W=6：4) were estimated, respectively. Firstly, the effects of solvent parameters (polarizability, polarity and charge distribution) on the configuration were considered.

Table S8 Solvent parameters of THF, *i*PrOH and H_2O.

***** Eps: static dielectric constant; Epsinf: dynamic dielectric constant; H-Bond Acidity:Abraham

	Eps*	**Epsinf *** (25℃)	**H-Bond Acidity***	**H-Bond Basicity***	**Surface Tension**	**Carbon Aromaticity**	**Electronegative Halogenicity**
THF	7.425	1.972339	0.00	0.48	39.44	0.000	0.000
*i*PrOH	19.26	1.891175	0.33	0.56	30.13	0.000	0.000
H_2O	78.35	1.775023	0.82	0.35	103.63	0.000	0.000

acidity; H-Bond Basicity: Abraham basic; Surface Tension at Interface: cal/mol/A^2.

The parameters of mixed solvents could be estimated as follow:

THF/water=3:7

Eps=7.4257/4.5+(3.5/4.5)*78.355=62.5929

Epsinf=1.972339/4.5+(3.5/4.5)*1.775023=1.818871

HBondAcidity=(3.5/4.5)*0.82=0.637778

HBondBasicity=0.48/4.5+(3.5/4.5)*0.35=0.378889

SurfaceTensionAtInterface=39.44/4.5+(3.5/4.5)*103.63=89.36556

CarbonAromaticity=0.000

ElectronegativeHalogenicity=0.000

iPrOH /water=6:4

Eps=0.6*19.264+0.4*78.355=42.9004

Epsinf=0.6*1.891175+0.4*1.775023=1.8447142

HBondAcidity=0.6*0.33+0.4*0.82=0.526

HBondBasicity=0.6*0.56+0.4*0.35=0.476

SurfaceTensionAtInterface=0.6*30.13+0.4*103.63=59.53

CarbonAromaticity=0.000

ElectronegativeHalogenicity=0.000

If only Eps and Epsinf were considered, the configurations and molecular energies of both R14 and RL7 in mixed solvents could be estimated as follow:

Table S9 Calculation results of molecular energy of R14 and RL7 in mixed solvents.

THF/water 3:7		**E_{elec}** (a.u.)	**RE** (kcal/mol)	**E_{elec}+ZPE** (a.u.)	**RE(+ZPE)** (kcal/mol)	**G** (a.u.)	**RG** (kcal/mol)
A2B1-	R14	-	0.000	-	0.000	-	5.609
A3B3-	R14	-	4.150	-	4.398	-	11.669
A1B1-	RL7	-	6.908	-	5.050	-	0.000
A2B2-	RL7	-	7.126	-	5.537	-	0.073
***i*PrOH/water 6:4**		**E_{elec}** (a.u.)	**RE** (kcal/mol)	**E_{elec}+ZPE** (a.u.)	**RE(+ZPE)** (kcal/mol)	**G** (a.u.)	**RG** (kcal/mol)
A2B1-	R14	-	0.000	-	0.000	-	5.686
A3B3-	R14	-	4.162	-	4.403	-	11.731
A1B1-	RL7	-	6.849	-	4.979	-	0.000
A2B2-	RL7	-	7.070	-	5.466	-	0.104

If all solvent parameters were considered, the configurations and molecular energies of both R14 and RL7 in mixed solvents could be estimated as follow:

Table S10 Calculation results of molecular energy of R14 and RL7 in mixed solvents.

THF/water 3:7		**E_{elec}** (a.u.)	**RE** (kcal/mol)
A2B1-3A2B1	R14	-2488.59763934	0.000
A3B3-3	R14	-2488.59608498	0.975
A1B1-2	RL7	-2488.56371331	21.289
A2B2-2	RL7	-2488.56395933	21.135
***i*PrOH/water 6:4**		**E_{elec}** (a.u.)	**RE** (kcal/mol)
A2B1-3A2B1	R14	-2488.61502369	0.000
A3B3-3	R14	**-2488.61185335**	**1.989**
A1B1-2	RL7	**-2488.58681198**	**17.703**
A2B2-2	RL7	**-2488.58680744**	**17.706**

Therefore, the A2B1-3A2B1 R14 configuration should be the optimized one in both mixed solvents due to the lowest RE values.

In THF/water=3:7 system:

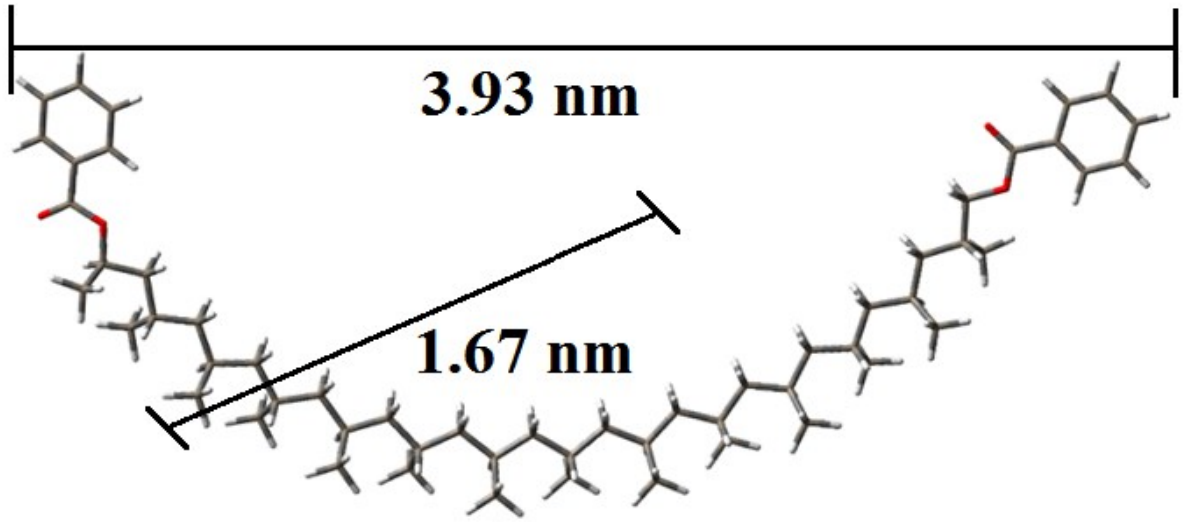

In iPrOH/water 6:4 system:

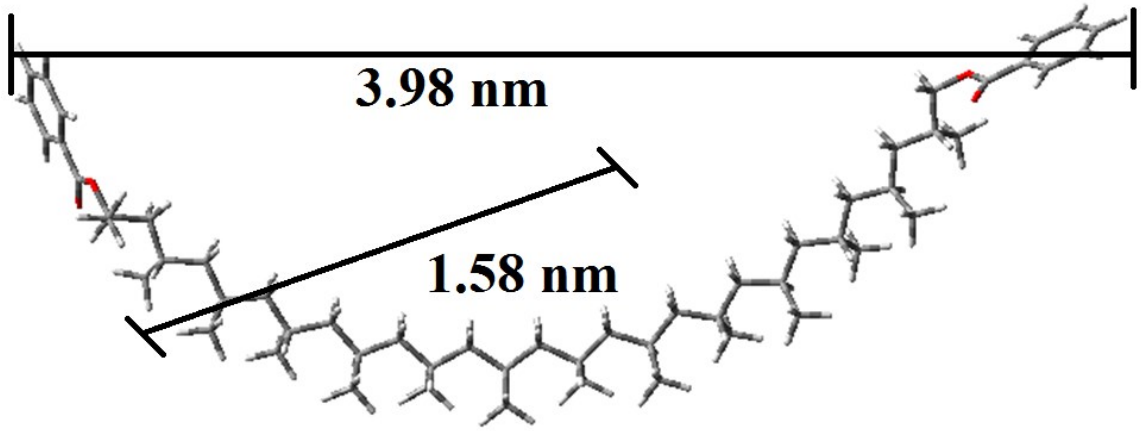

Table S11 Enantioselective separation of reported supramolecular chiral nanomaterials towards chiral molecules.

Supramolecular chiral nanomaterials	**Small chiral molecules**	***ee* %**	**Ref.**
Chiral porous interpenetrating polymer networks	racemic α-glucose	35%	S1
Chiral Cu surface	aspartic acid	37-39 %	S2
Chiral metal-organic frameworks	racemic sulfoxides	16.9-46.8 %	S3
Chiral Au nanoparticles	propylene oxide	No value	S4
Helical silica nanotube-graphene hybrids	amino acid derivatives	No value	S5

Table S12. Enantiomeric excess (*ee* (%)) of the prepared chiral assemblies for different racemic organic acids.

Chiral assemblies	***L*-/*D*-CSA**	***L*-/*D*-alanine**	***L*-/*D*-phenylalanine**
left-handed DMNDB nanowires	4.0%	2.5%	3.6 %
left-handed DMNDB/TANI nanowires	30.5%	15.6%	16.7%
right-handed DMNDB xerogel	2.7%	4.0%	3.4 %
right-handed DMNDB/TANI xerogel	22.6%	15.8%	14.6%

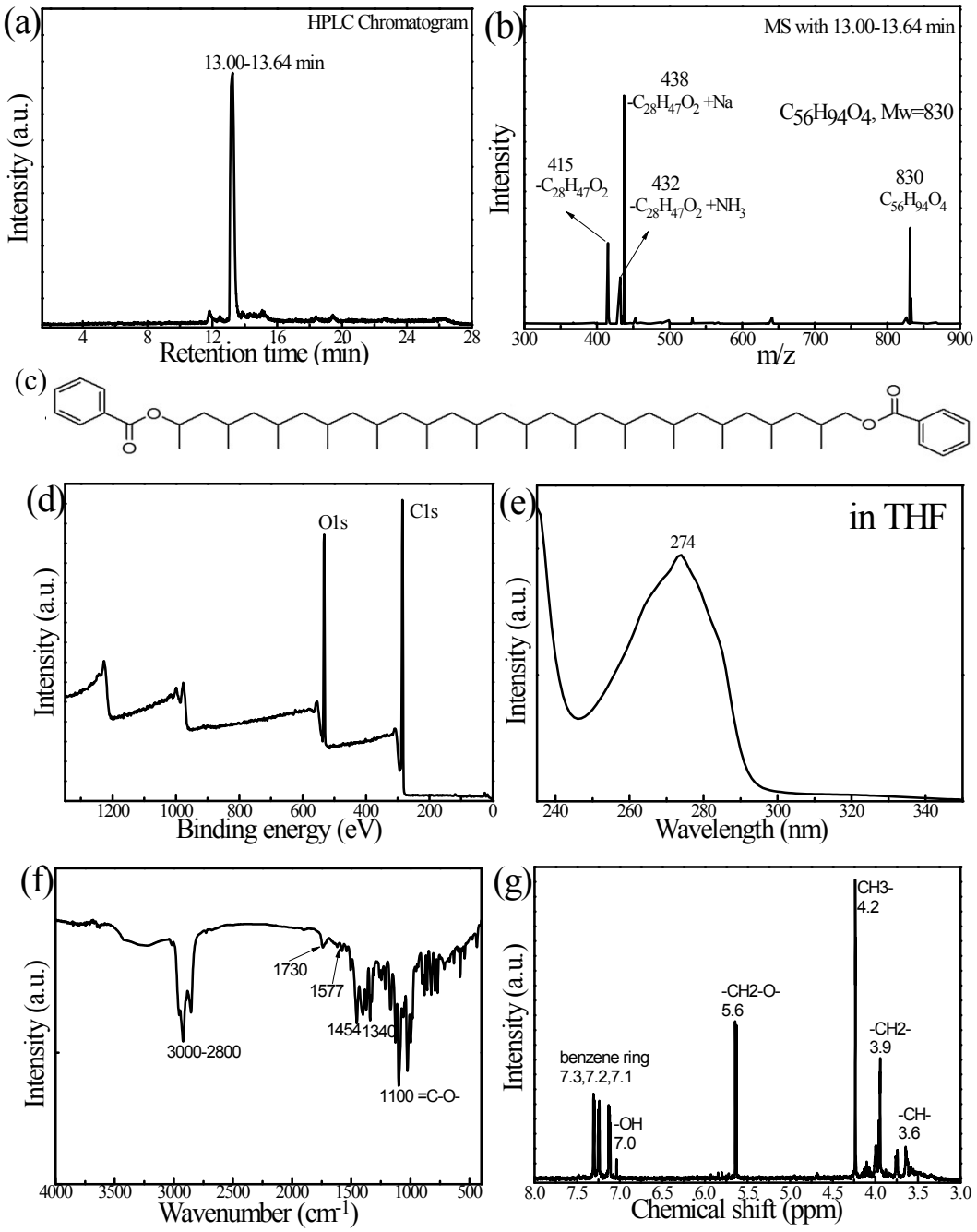

Fig. S1 (a) HPLC chromatogram of the matter abstracted from sheared polypropylene resins, (b) MS of the maximum HPLC component of the matter with retention time of 10.23-10.29 min. (c) a possible molecular structure of the studied specie. (d) XPS, (e) UV-vis, (f) FTIR and (g) ^{1}H NMR of the specie.

For determining the molecular structures of propylene oligomer, high-performance liquid chromatography spectrometer (HPLC) technique is employed to separate the obtained product. A

major HPLC peak with the retention time of 13.00-13.64 min is observed and analyzed by MS spectrometer equipped onto HPLC (b) to be $C_{56}H_{94}O_4$ with M_w=834 m/z, which is reasonably inferred to be 4,6,8,10,12,14,16,18,20,22,24,26-dodecamethylnonacosane-2,28-diyl dibenzoate, simplified as DMNDB whose molecular structure is displayed in (c). Element analysis results (Table S1) indicate that the measured values of every elements in the material are basically identical to these theoretical values according to its molecular structure, proving the molecular structure of DMNDB. XPS survey spectrum of the product displays only two main peak C_{1s} and O_{1s}, also attesting that the product just contains carbon and oxygen elements. The UV-vis result of the product dissolved in THF (e) gives an absorption at 250-290 nm, hinting the presence of the benzene rings in the molecular structures of the product. In the FTIR data (f), three strong peaks in the range of 2800-3000 and 1340 cm^{-1} were attributed to the stretching and in-plane C-H flexural vibration modes of methyl, methylene and methine groups,[S6] attesting that propylene act as a repetitive unit in the oligomers. Two absorption bands at around 1730 and 1100 cm^{-1} should be due to the stretching vibrations of C=O and C-O-C groups, respective, while the weak peak near 1577 and 1450 cm^{-1} could be assigned to the C=C and skeleton stretching modes of the benzenoid rings, respectively,[S7] thus. The above FTIR data suggest again that the as-obtained product contains propylene repetitive units and benzoyl peroxide (BPO) segment. The wide peaks in the range of 3220-3290 cm^{-1} might be due to some free OH^- groups probably dissociated by water molecules. Fig. (g) shows the ^1H NMR spectrum of the obtained product dissolved in D_6-acetone. The signals with chemical shifts at 7.1, 7.2 and 7.3 ppm are associated with those protons of H atoms directly bonded to aromatic rings, indicative of mono-substituted benzene ring.[S8] The signals at 4.2, 3.9 and 3.6 ppm should correspond to those protons of H atoms in the methyl, methylene and methine groups, respectively, while the chemical shift at about 5.6 ppm might be assigned to the protons in the $-CH_2-O-$ groups.[S9] These NMR results attested again that the product is composed mainly of DMNDB. The commercial PP resins may contain more propylene oligomer with other molecular structure or higher molecule weight, but it is favorable for such regular tetradecyl oligomer to disband from the resin surface into organic solvent.

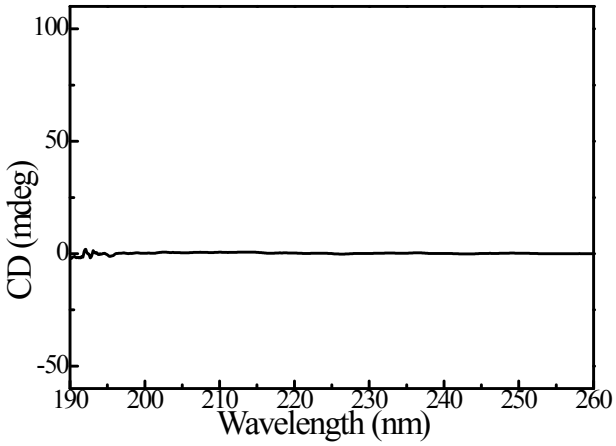

Fig. S2 CD spectrum of the DMNDB dissolved in THF with the experimental conditions: [DMNDB]=2.4 g/L, 20 °C. Although the DMNDB molecule has asymmetric carbon atoms in its molecular structure (Scheme 1), the CD spectrum of this matter dissolved in THF shows only noise background curve, which might be ascribed to that the localized chirality is far from the chromophore region similar to other molecule.[S10]

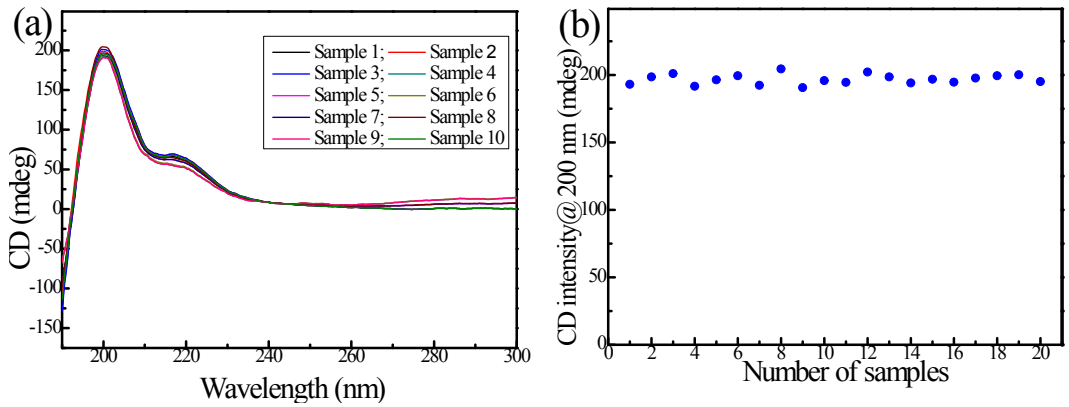

Fig. S3 (a) CD spectra of 10 left-handed nanowires samples prepared under the identical conditions. (b) Statistical distributions of CD intensity at 200 nm obtained from 20 samples. The self-assembly experimental conditions for the DMNDB nanowires: [DMNDB]= 2.4 g/L, THF/water volume ratio=3:7, 20 ^{o}C, pH=7.

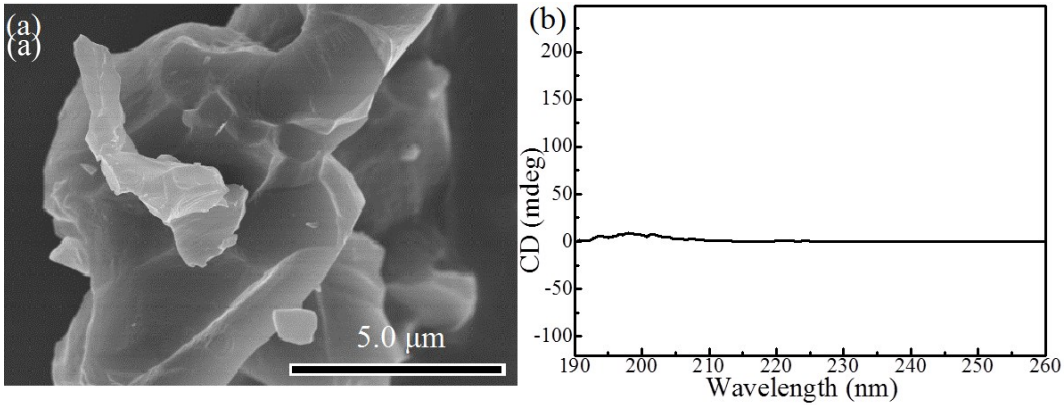

Fig. S4 (a) FESEM image and (b) CD spectrum of DMNDB assemblies formed with the self-assembly experimental conditions: [DMNDB]= 2.4 g/L, THF/water volume ratio=2:8, 20 ^{o}C, pH=7.

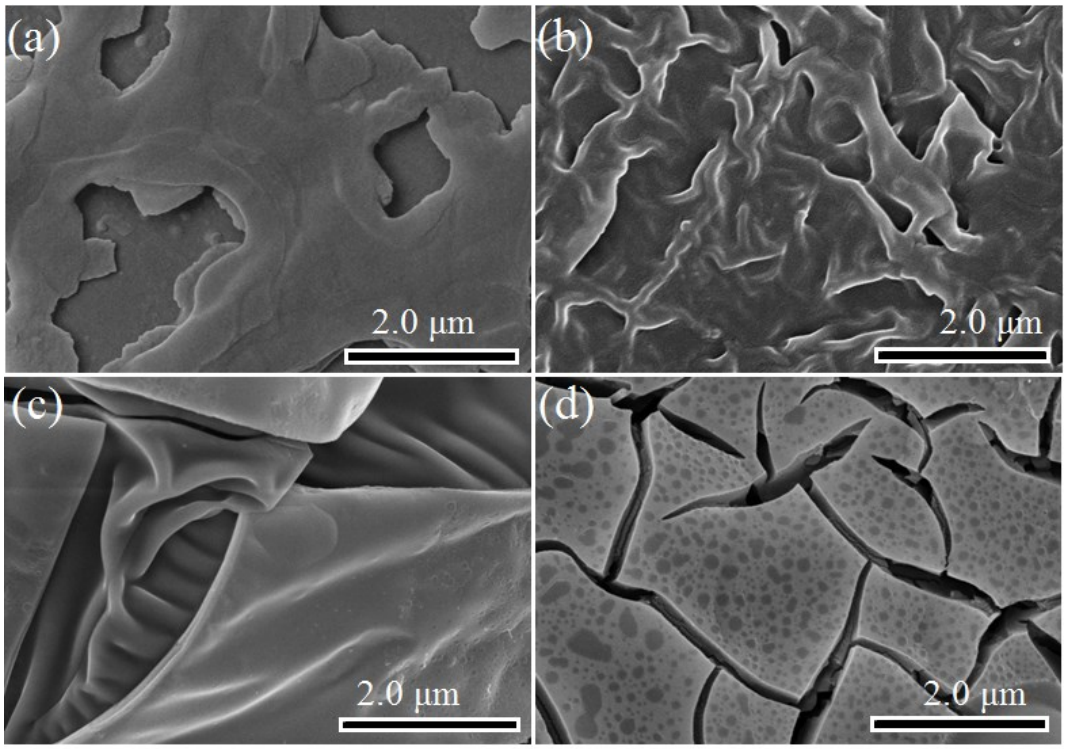

Fig. S5 FESEM image of DMNDB assemblies formed in (a) dimethyl sulfoxide (DMSO)/water, (b) N,N-dimethylformamide /water, (c) acetone/water, (d) *i*PrOH/water. Other experimental conditions: [DMNDB]= 2.4 g/L, organic solvent/water volume ratio=3:7, 20 ^{o}C, pH=7.

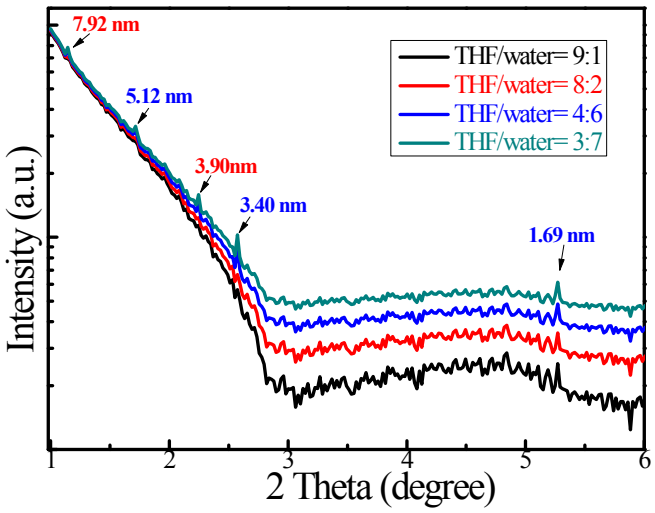

Fig. S6 Small-angle XRD patterns of the nanoassemblies formed with different THF/water volume ratios (9:1, 8:2, 4:6 and 3:7). Other self-assembly experimental conditions: [DMNDB]= 2.4 g/L, 20 ^{o}C, pH=7.

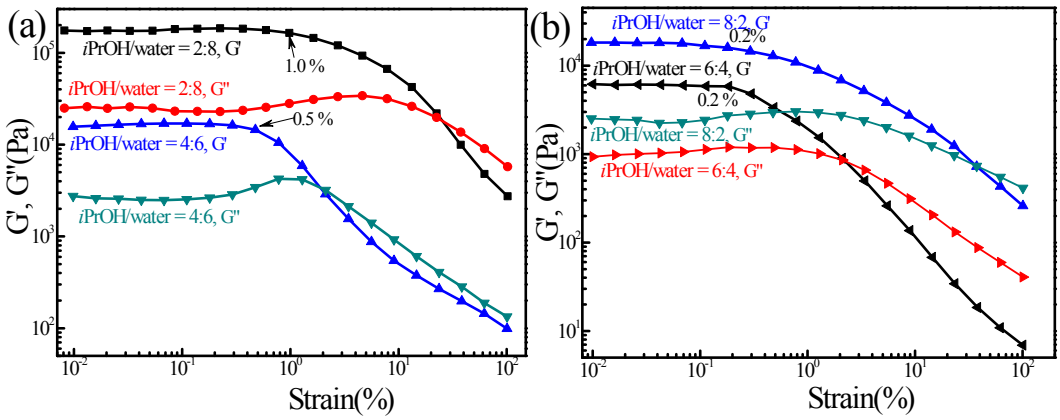

Fig. S7 (a, b) Rheological measurement of strain sweep at frequency of 1 rad^{-1} over a range of strain of 0.01 %-100% of mixed-solvent gel with different *i*PrOH/water ratio: (a) 2:8 and 4:6; (b) 6:4 and 8:2. Other preparation conditions: [DMNDB]= 4 g/L, 20 ^{o}C, pH=7.

For the gel with the *i*PrOH/water ratio of 2:8, the modulus of elasticity (G') maintains unchanged at the beginning strain (<1.0%), after that, G' gradually decrease with the strain increasing. This indicates that the gel obtained at this ratio could keep mechanics strength for the strain <1.0%, and the strain=1.0% is considered to be key point. The key points for the gels formed at the *i*PrOH/water ratio of 4:6, 6:4 and 8:2, are found to be 0.5%, 0.2% and 0.2%, respectively.

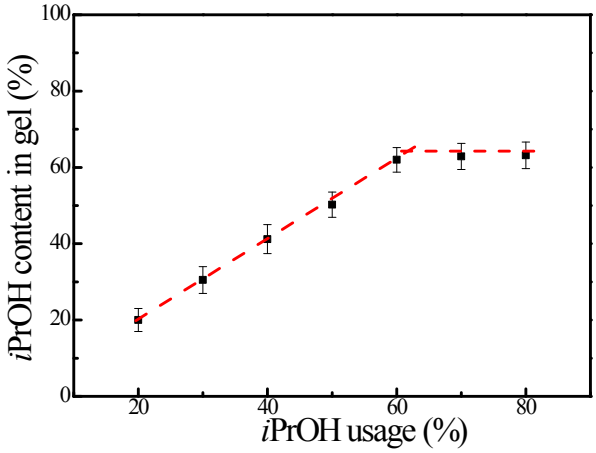

Fig. S8 *i*PrOH content in gel samples changing with the *i*PrOH usage in the preparation. For measuring the *i*PrOH content in gel sample, the mixed solvent immobilized in gel was abstracted by membrane filter method. And then the alcohol content in the filtrate was tested using Headspace Gas Chromatography (7890A-7697A, Agilent) technique and estimated through a standard curve method.

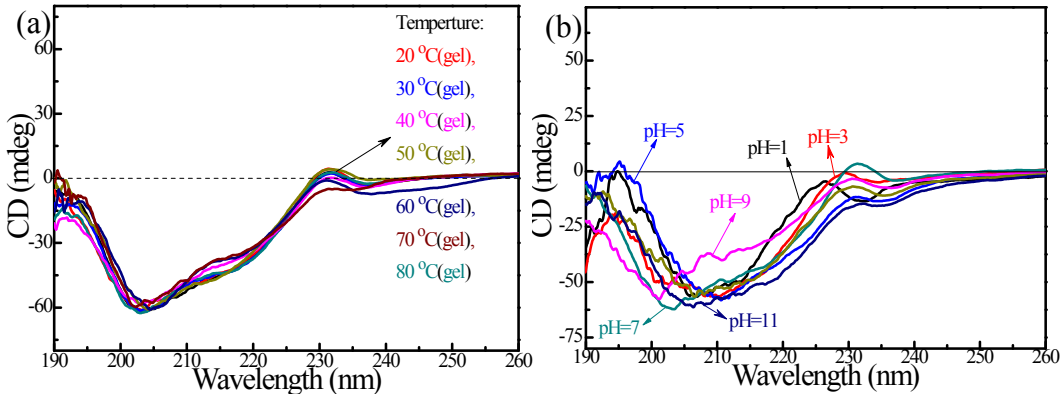

Fig. S9 (a) CD spectra of the DMNDB gel sample under different temperatures with other preparation conditions: [DMNDB]= 4 g/L, *i*PrOH/water ratio = 6:4 (v/v), pH=7. (b) CD spectra of the DMNDB gel sample under different pH with other preparation conditions: [DMNDB]= 4 g/L, *i*PrOH/water ratio = 6:4, 20 °C.

In traditional preparation of supramolecular gel, small molecule gelators were firstly dissolved in a solvent by heating, and then form cross-linked nanostructure networks by cooling.[S9,S11] Different from the traditional method, DMNDB gel was produced by directly mixing these twisted nanowires into *i*PrOH/water system. Since these stabile nanostructures have been pre-formed, such DMNDB gel sample might exhibit high environment stability. Indeed, the obtained gel possess well thermal stability, as evidenced from negligible changes in CD spectra of the DMNDB gel when heated from 20 °C to 80 °C. As known, thermodynamic control on the supramolecular chiral assembly usually generates dynamic helical structures that cannot keep their supramolecular chirality in solution, while the kinetic control often results in stable helical structures with obvious supramolecular chirality. In this work, the DMNDB gel retains their optical properties even at a high temperature of 80 °C, meaning that the self-assembly of DMNDB in gel should be under kinetic control rather than thermodynamic control.[S12,S13]

Under different solution pH (1-13), the gel sample always displays the negative Cotton effects with a similar intensity, whose main CD signal varies in the rang of 200-220 nm. This result states that the electrostatic interactions should be absent in the supramolecular chiral gel. Thus, the supramolecular chiral gel of DMNDB have fine environment stability towards temperature and system acidity.

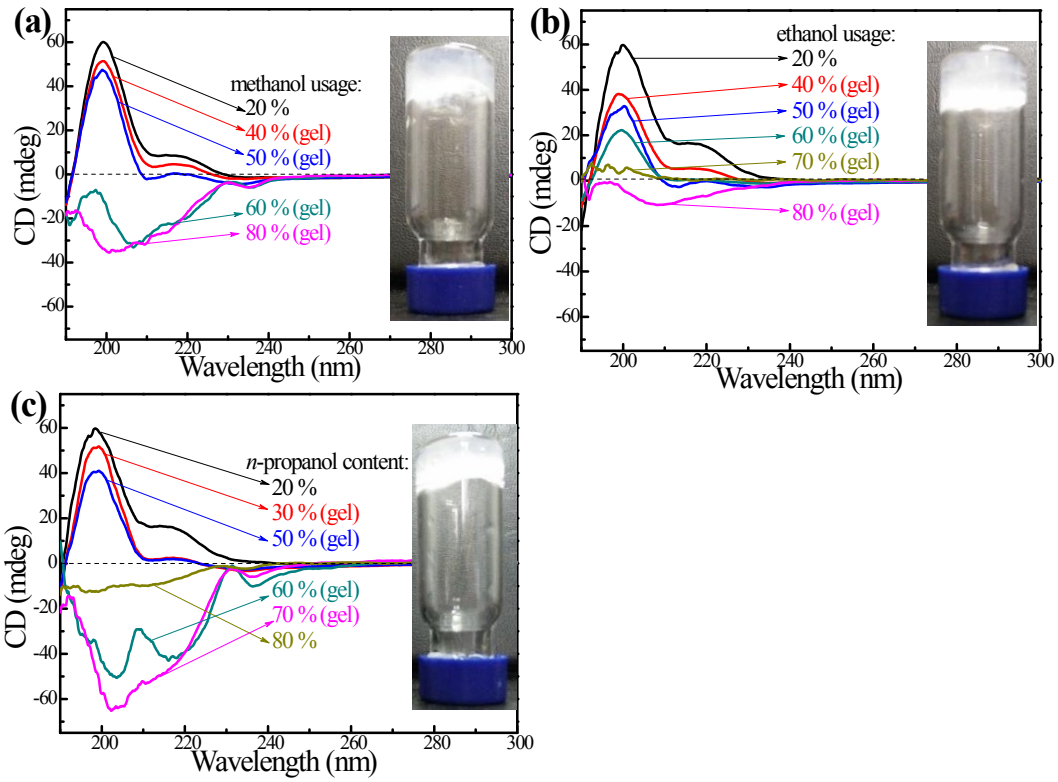

Fig. S10 CD spectra of DMNDB gel samples formed in (a) methanol/water, (b) ethanol/water, and (c) *n*-propanol/water system with different alcohol contents. Inserts gives optical photographs of the corresponding samples with alcohol/water volume ratio (5:5). Other preparation conditions: [DMNDB]= 4 g/L, 20 ^{o}C, pH=7.

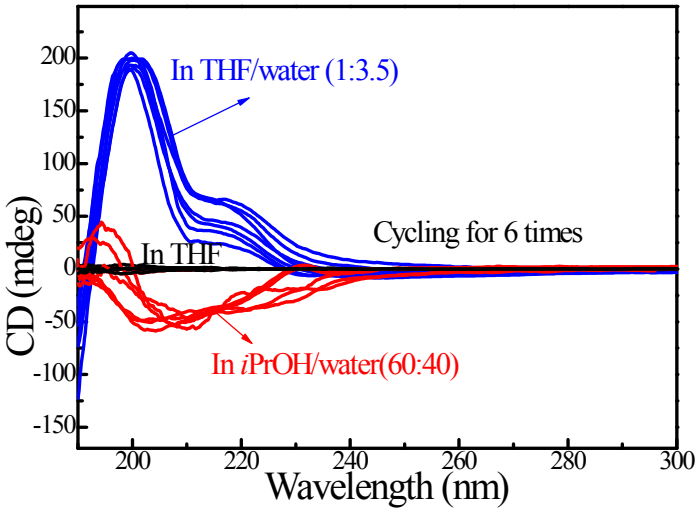

Fig. S11 CD spectra of DMNDB assemblies formed in THF/water and *i*PrOH/water systems for 6 cycles. The self-assembly experimental conditions of twisted nanowires: [DMNDB]= 2.4 g/L, THF/water ratio=3:7, 20 °C, pH=7; The preparation conditions of chiral gel: [DMNDB]= 4 g/L, *i*PrOH/water ratio = 6:4, 20 °C, pH=7.

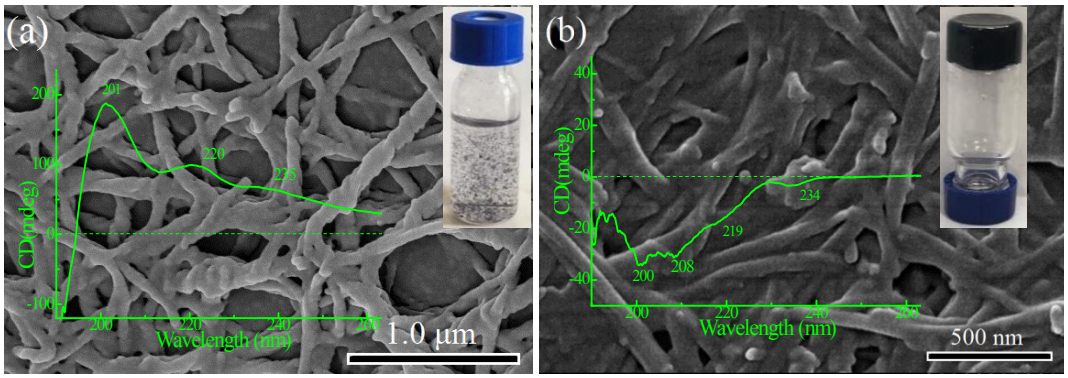

Fig. S12 (a) FESEM image and CD spectrum of complex DMNDB/tetraaniline (TANI) assemblies formed in THF/water system with the self-assembly experimental conditions: [DMNDB]= 2.4 g/L, [TANI]=0.75 g/L, THF/water ratio=3:7, 20 °C, pH=7. (b) FESEM image and CD spectrum of complex DMNDB/TANI xerogel formed in *i*PrOH/water system with the preparation conditions: [DMNDB]= 3.05 g/L, [TANI]=0.95 g/L, *i*PrOH/water ratio = 6:4, 20 °C, pH=7.

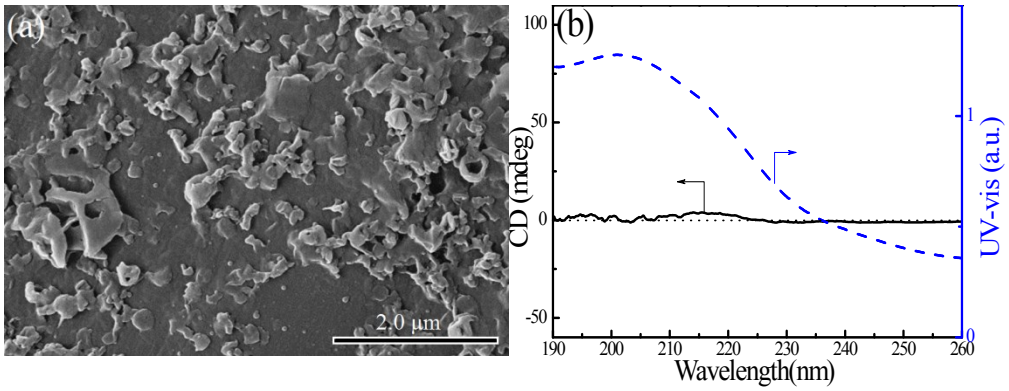

Fig. S13 (a) FESM image of TANI assemblies in THF/water system. (b) CD and UV-vis spectra of TANI assemblies dispersing in water. The self-assembly experimental conditions: [TANI]=2.4 g/L, THF/water volume ratio=3:7, 20 ^{o}C, pH=7.

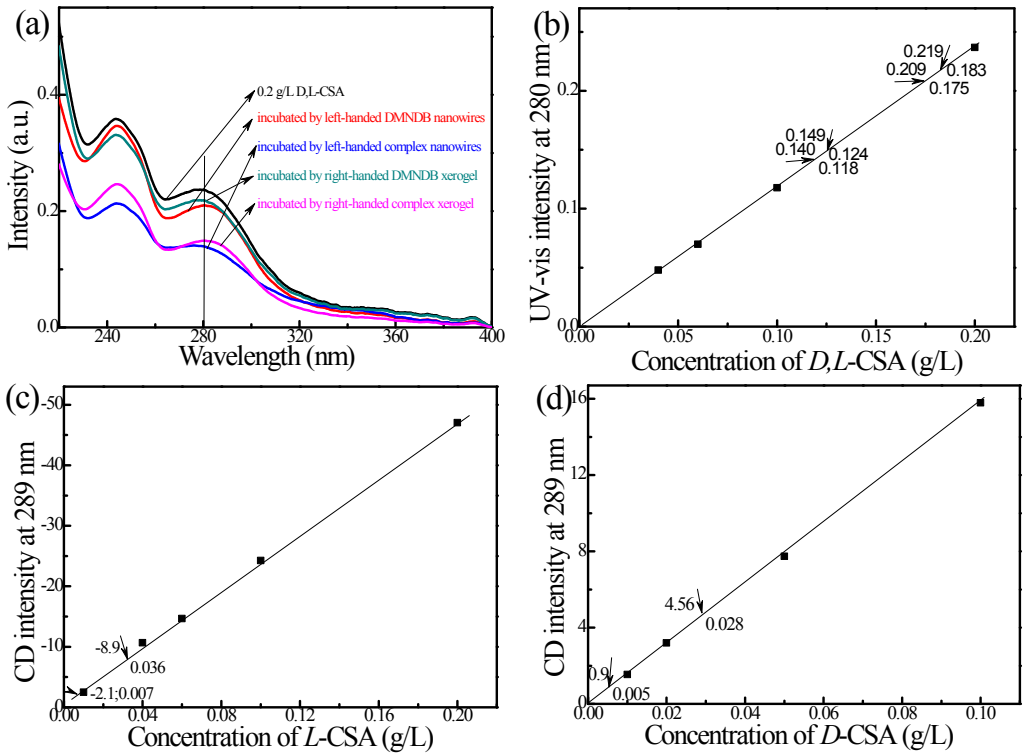

Fig. S14 (a) UV-vis spectra of 1:1 mixture of *L*-/*D*-camphorsulfonic acid (0.2 g/L) and filtrates incubated by left-handed DMNDB nanowires and DMNDB/TANI complex nanowires, right-handed DMNDB xerogel and DMNDB/TANI complex xerogel. (b) UV-vis intensity of racemic camphorsulfonic acid (CSA) at 280 nm *versus* the total concentration ($C_{L\text{-CSA}}$+$C_{D\text{-CSA}}$). (c) CD intensity of *L*-CSA at 289 nm *versus* its concentration ($C_{L\text{-CSA}}$). (d) CD intensity of *D*-CSA at 289 nm *versus* its concentration ($C_{D\text{-CSA}}$).

REFERENCES

(S1) Liang, J.; Deng, J. A Chiral Interpenetrating Polymer Network Constructed by Helical Substituted Polyacetylenes and Used for Glucose Adsorption. *Polym. Chem.* **2017**, *8*, 1426−1434.

(S2) Yun, Y.; Gellman, A. J. Chiral Mesoporous Spherical Silica Enantioselective Separation on Naturally chiral Metal Surfaces: *D, L*-Aspartic Acid on Cu(3,1,17)$^{R\&S}$ Surfaces. *Angew. Chem. Int. Ed.* **2013**, *52*, 3394−3397.

(S3) Zhang, J.; Li, Z.; Gong, W.; Han, X.; Liu, Y.; Cui, Y. Chiral DHIP-Based Metal-Organic Frameworks for Enantioselective Recognition and Separation. *Inorg. Chem.* **2016**, *55*, 7229−7232.

(S4) Shukla, N.; Bartel, M. A.; Gellman, A. J. Enantioselective Separation on Chiral Au Nanoparticles. *J. Am. Chem. Soc.* **2010**, *132*, 8575−8580.

(S5) Jung, J. H.; Moon, S. J.; Ahn, J.; Jaworski, J.; Shinkai, S. Controlled Supramolecular Assembly of Helical Silica Nanotube–Graphene Hybrids for Chiral Transcription and Separation. *ACS Nano* **2013**, *7*, 2595−2601.

(S6) Geng, Y.; Wang, G.; Cong, Y.; Bai, L.; Li, L.; Yang, C. Shear-Induced Nucleation and Grwoth of Long Helices in Supercooled Isotactic Polypropylene. *Macromolecules* **2009**, *42*, 4751-4757.

(S7) Wang, Z.; Fan, X.; Wang, K.; Deng, H.; Chen, F.; Fu, Q.; Na, B. Ordered Long-Helical Conformation of Isotactic Polypropylene Obtained in Constrained Environment of Nanoclay. *Polym. Adv. Technol.* **2011**, *22*, 1375-1380.

(S8) Venancio, E. C.; Wang, P.-C.; MacDiarmid, A. G. The azanes: A class of material incorporating nano/micro self-assembled hollow spheres obtained by aqueous oxidative polymerization of aniline. *Synth. Met.* **2006**, *156*, 357−369.

(S9) Ding, Z.; Sanchez, T.; Labouriau, A.; Iyer, S.; Larson, T.; Currier, R.; Zhao, Y.; Yang, D. Characterization of Reaction Intermediate Aggregates in Aniline Oxidative Polymerization at Low Proton Concentration. *J. Phys. Chem. B* **2010**, *114*, 10337−10346.

(S10) Vedhanarayanan, B.; Naire, V. S.; Nair, V. C.; Ajayaghosh, A. Formation of Coaxial Nanocables with Amplified Supramolecular Chirality through an Interaction between Carbon Nanotubes and a Chiral pi-Gelator. *Angew. Chem. Int. Ed.* 2016, 55, 10345−10349.

(S11) Yu, G.; Yan, X.; Han, C.; Huang, F. Characterization of Supramolecular Gels. *Chem. Soc. Rev.* **2013**, *42*, 6697−6722.

(S12) Liu, G.; Sheng, J.; Wu, H.; Yang, C.; Yang, G.; Li, Y.; Ganguly, R.; Zhu, L.; Zhao, Y. Controlling Supramolecular Chirality of Two-Component Hydrogels by J- and H-Aggregation of Building Blocks. *J. Am. Chem. Soc.* **2018**, *140*, 6467-6473.

(S13) Liu, G.; Sheng, J.; Teo, W. L.; Yang, G.; Wu, H.; Li, Y.; Zhao, Y. Control on Dimensions and Supramolecular Chirality of Self-Assemblies through Light and Metal Ions. *J. Am. Chem. Soc.* **2018**, *140*, 16275-16283.